

1 **Seeing the light: Improving the usability of**
2 **fluorescence-guided surgery by adding an optimized**
3 **secondary light source**

4
5 Jonathan T. Elliott, PhD^{1,2,*}; Dennis J. Wirth, PhD²; Scott C. Davis, PhD²;
6 Jonathan D. Olson, MEng²; Nathan E. Simmons, MD¹; Timothy C. Ryken, MD,
7 MS¹; Keith D. Paulsen, PhD²; David W. Roberts, MD¹

8
9 1. Department of Surgery, Dartmouth-Hitchcock Medical Center, Lebanon, New Hampshire 03756

10 2. Thayer School of Engineering at Dartmouth, Hanover, New Hampshire 03755;

11
12 *Corresponding Author:

13
14 Prof. Jonathan T. Elliott
15 Assistant Professor of Surgery
16 Senior Scientist, TEC Program
17 Dartmouth-Hitchcock Medical Center
18 1 Medical Center Drive
19 Lebanon, NH 03756

20
21 Email: jonathan.t.elliott@dartmouth.edu

22 Tel: 603 650-1910
23
24

25 **Abstract**

26 **Background:** Tumors that take up and metabolize 5-aminolevulinic acid (5-ALA) emit bright pink
27 fluorescence when illuminated with blue light, aiding surgeons in identifying the margin of
28 resection. The adoption of this method is hindered by the blue light illumination, which is too dim
29 to safely operate under, and therefore, necessitates switching back and forth from white-light mode.
30 This paper examines the addition of an optimized secondary illuminant adapter (SIA) to improve
31 usability of blue-light mode without degrading tumor contrast.

32 **Methods:** We used color science methods to evaluate the color of the secondary illuminant and its
33 impact on color rendering index (CRI) as well as the tumor-to-background color contrast (TBCC).
34 A secondary illuminant adapter was built to provide 475-600 nm light the intensity of which can
35 be controlled by the surgeon and was evaluated in two patients.

36 **Results:** Secondary illuminant color had opposing effects on color rendering index (CRI) and
37 tumor to background color contrast (TBCC); providing surgeon control of intensity allows this
38 trade-off to be balanced in real-time. Experience in two cases suggests additional visibility adds
39 value.

40 **Conclusion:** The addition of a secondary illuminant may mitigate surgeon complaints that the
41 operative field is too dark under the blue light illumination required for 5-ALA fluorescence
42 guidance by providing improved CRI without completely sacrificing TBCC.

43

44 **Key Words:** 5-aminolevulinic acid, dynamic contrast-enhanced, fluorescein, fluorescence-guided surgery,
45 GBM, glioma, PpIX

46

47

48

49

50 **Declarations:**

51 *Funding:* NIH/NCI R00 CA190890, NIH/NCI RO1 NS052274

52 *Conflicts of interest/competing interests:* none.

53 *Availability of data and material:* upon request

54 *Code availability:* upon request

55 *Ethics approval:* Dartmouth IRB Study No. 00028077

56 *Consent to participate:* Written consent was obtained from all subjects.

57 *Consent for publication:* All authors consent to the publication of this work.

58 Introduction

59 Fluorescence guided surgery (FGS) is gaining popularity as a tool for improving extent of tumor
60 resection in high grade glioma (HGG) ¹⁻⁵. Currently, while there are a handful of approved fluorophores
61 that can be visualized intraoperatively, 5-aminolevulinic acid (5-ALA), which is converted to the
62 fluorophore protoporphyrin IX (PpIX) and preferentially accumulates in tumor cells, remains one of the
63 most popular. The quick adoption of 5-ALA is attributable to three factors: 1) It can be visualized directly
64 through compatible operating microscopes; 2) its near-monochromatic emission at 635 nm gives highly
65 saturated reddish-purple or purplish-pink signal that contrasts strongly with tissue reflectance under blue
66 excitation; 3) it is highly specific for high-grade glioma⁵, meningioma⁶ and metastasis². Recent studies
67 suggest 5-ALA contributes to improvements in disease free progression in HGG,⁷ and other tumors.⁸⁻¹²
68 Increased sensitivity of quantitative imaging methods¹³⁻¹⁵ may further expand the role of 5-ALA.

69 Interfering with the ease of use of 5-ALA by neurosurgeons, however, is the suboptimal
70 illumination of the surgical field under blue light conditions. Difficulty visualizing fine structure under
71 those conditions prevents many surgeons from performing the procedure while using fluorescence-
72 guidance, relegating the technology's role to intermittent assessment of the field, particularly at the
73 presumed end of resection. The importance of predictable and controlled illumination during surgery has
74 been recognized from the earliest days of modern scientific surgery—even before electricity was
75 available, surgery was performed on the top east-facing room in the early morning to maximize the
76 availability of natural light. Color is an interpretation, by human visual perception, of reflected or emitted
77 light spectra governed by the object's optical properties (scatter, absorption, and luminescence) and the
78 illuminant.¹⁶ The appearance of an object is determined by both the *white-point* of the illuminant and the
79 reflectance spectrum of the object, resulting in perceived color and lustre. Because a blue light illuminant
80 occupies a non-overlapping locus in the visible color space, it cannot adequately render tissue color, which
81 is heavily represented in the red, pink and yellowish-pink part of the visible color space. As a result, the
82 latter appears dark, cold, and tissue lacks its natural visual texture due to the absence of discernable color
83 variations; PpIX emission, however, occupies a locus along the line of purples, and appears as a vibrant
84 (saturated) reddish-purple or pinkish-purple color, as the 635 nm emission blends with the 405 nm
85 excitation.

86 Operating under blue illumination impacts surgeons' visualization of critical nerves and other
87 landmarks. Notably, even frank bleeding in the surgical field (an important clinical observation) is not
88 perceivable until enough blood covers a large enough area of the field to darken the blue-light illuminated
89 background. Despite these limitations, however, because of the intensity of color contrast between PpIX-
90 enhancing and non-enhancing tissue, the challenges in usability are often outweighed by the marked

91 improvements in tumor discrimination. Therefore, surgeons often switch between blue and white-light
92 illumination manually during the course of surgery.

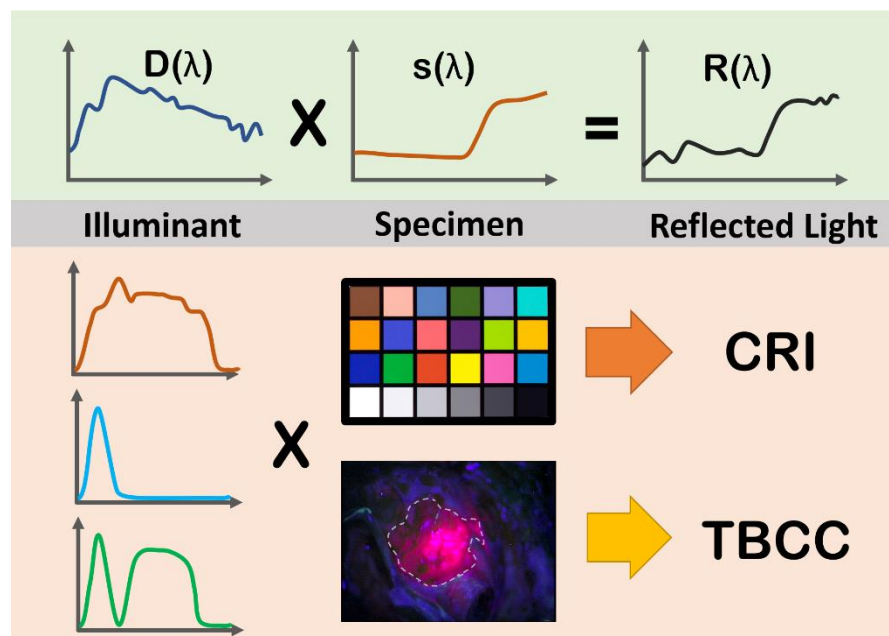
93 To overcome visual limitations of operating in blue light mode, while preserving the benefits of
94 PpIX emission afforded to tumor identification, we introduced a secondary illuminant into the surgical
95 field whose spectrum was optimized to achieve two competing goals: maximizing the contrast between 5-
96 ALA-enhancing tumor cells and the background, and maximizing the amount of contamination of the
97 excitation source and overlap with the PpIX emission peak. Specifically, we explored how the color of the
98 light spectrum added to the blue illumination enhanced the color of non-fluorescent tissue in the surgical
99 field (color rendering index) and affected the contrast between fluorescent tumor and non-fluorescent
100 background. Conceptually, the approach is illustrated in **Figure 1**.

101

102 **Materials and Methods**

103 *Color Theory*

104 What we perceive as color is a result of both the intrinsic properties of an object, and the properties of the
105 light used to illuminate it. Without light, we cannot see color, and under different types of illumination,
106 color appears differently. The dependency of illumination on the evaluation or communication of color
107 has led to the development of standardized illuminants such as D65, the spectral power distribution of
108 daylight in the Northern European sky. Formally, we can define the spectrum of light reflected from the
109 surface of a specimen, $R(\lambda)$, as the product of the illuminant spectrum, $D(\lambda)$, and the intrinsic spectral
110 reflectance of the object, $s(\lambda)$. The top row of **Figure 1** summarizes this formalism. To understand the
111 effect of the illuminant on the light reflected off the surface of a specimen, we used a standardized
112 illuminant and hyperspectral imaging camera to obtain the pixel-by-pixel spectral reflectance of a
113 ColorChecker card and of the surgical field from nine patients (see subsection “Clinical Study” below).
114 These intrinsic spectra were convolved with different illuminants to obtain reflection spectra specific to
115 these lighting conditions. To quantitatively assess these effects, two metrics were used: (1) the color
116 rendering index (CRI), which measures the ability of a light source to render the ColorChecker test colors
117 faithfully in comparison to the standard D65 light source,¹⁷ and the tumor to background color contrast
118 (TBCC), which measures the average distance (Euclidean) between the colors in the tumor and
119 background regions of the image. These two metrics were used in simulations to optimize the secondary
120 light source. **Figure 1** summarizes this approach, and additional technical details are provided in the
121 Online Content.



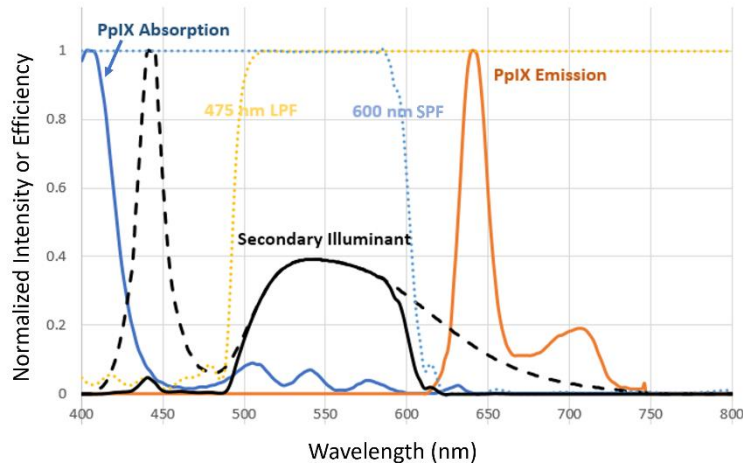
122

123 **Figure 1.** Perceived color of reflected light, $R(\lambda)$, is a result of the intrinsic spectral reflectance of an object, $s(\lambda)$,
124 and the spectral density of the illuminant, $D(\lambda)$. Different illuminants can result in dramatically different color
125 renderings—measured by the color rendering index (CRI). In the context of surgical guidance, the tumor-to-
126 background color contrast (TBCC) is also affected by the illuminant.

127

128 *Secondary Light Source Instrumentation*

129 A Pentero BLUE400 operating microscope (Zeiss) was fitted with a custom designed and 3D printed
130 secondary illuminant adapter (SIA), that attaches to the bottom of the microscope head via the Zeiss
131 standard dovetail interface (Fig. ESM1, Online Content). The SIA contained a 7-W Cree XM-L T4
132 650LM LED emitter (SKU 1685402, FastTech.com), with color temperature range of 3700-5000 K,
133 connected to a variable-intensity LED driver (LEDD1B, Thorlabs, Inc., Newton, NJ). Two filters (short-
134 pass filter, SPF, and long-pass filter, LPF) were placed between the LED board to achieve the desired
135 bandwidth of light (**Figure 2**) and a plano convex lens to expand the profile of the light. At a 300-mm
136 working distance, when the dial on the LED driver was set to 9, maximum power meter density was
137 measured as 14.6 mW/cm². For the 8 cm radius spot size at 300 mm distance, the illuminance was
138 approximately 40,000 lux.



139

140 **Figure 2.** The absorption (solid blue line) and emission (solid orange line) spectra of PpIX along with the LED
141 spectrum (dashed line) and the portion that passes through the long-pass filter (LPF, yellow dotted line) and short-
142 pass filter (SPF; blue dotted line) forming the secondary illuminant (black line).

143

144 *Clinical Study*

145 All study procedures were approved by Dartmouth's IRB (Study No. 00028077; ClinicalTrials.gov
146 NCT02191488). Nine surgical patients with operable brain tumors, presenting between September 2014
147 and August 2015, provided informed consent before the surgery. Three hours before surgery they were
148 administered 20 mg/kg of ALA (DUSA Pharmaceuticals, Tarrytown, NY), used off-label under NDA
149 208630 since the oral route of administration was not approved in the US at the time of the study.
150 Craniotomy was performed using navigation (StealthStationS7, Medtronic Navigation, Inc., Louisville,
151 CO). Upon visualization of tumor and PpIX emission, sequential images under white-light and blue-light
152 were acquired from four locations. Video and images acquired using the SIA were obtained under the
153 same protocol following an IRB-approved planned deviation and a subsequent approved modification to
154 include the SIA as a new non-significant risk (NSR) device. Following sequential white-light and blue-
155 light imaging, video was acquired while the LED driver dial was turned up and down, to illustrate the
156 changing contrast provided by the SIA.

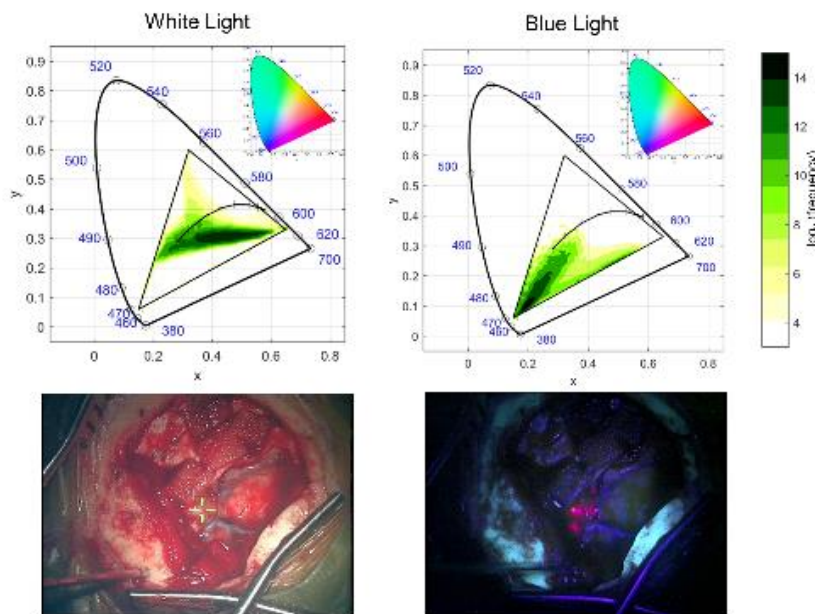
157

158 **Results**

159 *Characterization of Conventional Operating Microscope Illumination Modes*

160 Thirty-six pairs of images from nine patients were obtained and characterized to determine the color
161 gamut (*i.e.*, the range of colors represented across images of a particular group). **Figure 3** presents the
162 color gamuts under white light and blue light illumination within the cranial windows as probability
163 density functions that a particular pixel will have a particular chromaticity. White light views of the

164 surgical field are strongly weighted in the red to yellowish-pink field whereas the Blue images show a
165 locus in the opposing side of the color space. From these chromaticity diagrams, it is evident the change
166 in illuminant from white to blue has a dramatic effect on the reflected color, represented as chromaticity
167 in these maps. Pixels that represent a wide range of red, pink and pinkish-yellow under a standard
168 illuminant are compressed into the bottom left part of the chromaticity map, rendering them much less
169 distinguishable.

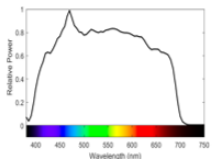
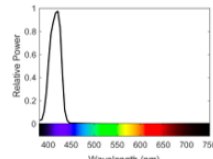
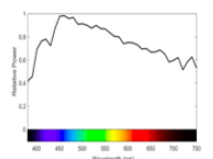
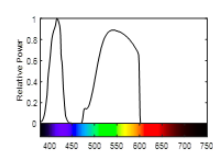


170
171 **Figure 3.** The probability density map of chromaticity calculated for thirty six pairs of intraoperative images under
172 white-light and blue-light illumination. The top row shows CIE 1931 chromaticity diagrams with the color gamut
173 indicated by the probability density map. Inset, a reference chromaticity map showing all visible colors is provided
174 for reference. The bottom two images show representative white-light and blue-light images taken from the set of
175 thirty-six pairs.

176
177 Given the dramatic impact that the choice of illuminant has on the appearance of tissue, it is therefore not
178 surprising that the FDA has guidelines for what type of lighting is used in the operating room. **Table 1**
179 summarizes the key characteristics of light sources used in surgery; the CIE D65 standard illuminant is
180 included for comparison. For each characteristic, values recommended by the FDA, found in the draft
181 IEC standard 60601-2-41/Ed1, are listed as well. The Pentero white-light is optimized to FDA guidelines
182 with a spectrum approximating daylight (D65 CIE Standard). A hot mirror reduces transmitted light
183 beyond 700 nm avoiding unnecessary energy deposition. The Pentero BLUE400 mode applies a 435 nm
184 on the white-light source, while simultaneously increasing the source power by 3.5 fold to ensure
185 adequate irradiance. The resulting monochromatic spectrum is unable to accurately render colors, and its

186 chromaticity coordinates approach the spectral locus of the 1931 x,y chromaticity space. One of the most
 187 intuitive ways to describe a light source is by its warmth or coldness—a reference to the physics concept
 188 that black, non-reflective objects (i.e., ‘black bodies’) emit light when heated based on their temperature.
 189 As an object is heated, it’s chromaticity can be traced on the chromaticity map as an arc moving from
 190 warm to cool colors. This Planckian Locus, as it is called, intersects only red, orange yellow, white and
 191 bluish white regions of chromaticity space (**Figure 3**). Therefore, while the other three light sources have
 192 well-defined color temperatures, the saturated blue Pentero source is said to have a temperature of
 193 infinity. Given the human eye is relatively insensitive to blue light, its luminance (which is a function of
 194 both the fluence and the wavelength-dependent efficiency of the vision system) falls below the FDA
 195 guidelines for surgical lighting. Additionally, the BLUE400 mode has poor color rendering and low
 196 luminance, representing key challenges for surgeons when operating in this mode.
 197

198 **Table 1** Spectral characteristics of light sources used in surgery, the D65 daylight CIE reference spectrum, and the
 199 combined light source evaluated here. Spectrum of both light sources, as measured by spectrometer. FDA
 200 guidelines for each characteristic are provided in the first column. Values outside of the guidelines are highlighted in
 201 red.

Characteristic (FDA guidelines)	Pentero White Light	Pentero Blue Light	D65 (Northern Europe Daylight)	Pentero Blue Light + Secondary Illuminant
Spectrum				
Color Temperature (K) 3010-6886 K	5,709.6	∞	6,503.6	5,739.4
Chromaticity coordinates (x,y) 0.35 (0.31-0.42), 0.37 (0.31-0.42)	0.33, 0.34	0.16, 0.03	0.313, 0.329	0.322, 0.516
Color Rendering Index > 85	97	< 0	100	32
Luminance 40,000 – 160,000 lux	70,000 lux	16,000 lux [†]	120,000 lux	16,000 lux (blue) + 40,000 lux (green)
Light Source (Tungsten/LED)	Tungsten Xenon Arc Lamp	Filtered Tungsten Xenon Arc Lamp	Sunlight	Filtered Xenon Lamp + Filtered CREE XM-L LED

[†] Estimated by converting mW/cm² measured by power meter to luminance using luminous intensity equation.

202
203

204 *Effect of Secondary Illuminant Addition on Color Rendering Index and Tumor Contrast*

205 To understand how secondary illuminant selection influences the color rendering index (CRI), a
206 key characteristic in FDA guidelines and quantitative assessment of how well colors are rendered by an
207 illuminant, experiments were obtained using a ColorChecker—an industry-standard card containing 24
208 color squares representative of the typical colors observed in the natural world. The full details of this
209 experiment are provided in the Online Content, but the salient points are summarized here.

210 Hyperspectral images of the ColorChecker card (X-Rite, Inc., Grand Rapids, MI) acquired under
211 white-light and blue-light illumination were used to evaluate the effect of varying intensity, short-pass
212 and long-pass filter selection of the secondary illuminant. As expected, CRI decreased monotonically
213 when the short-pass filter center wavelength was decreased, making the light more blue and narrower.
214 The worst filter combinations occur with narrow bands of light centered around 450 nm and 575 nm. For
215 CRI, the best bandwidth of light to add to the blue illumination spans the 475-650 nm range. In this case,
216 the CRI approaches the FDA guideline of 85.

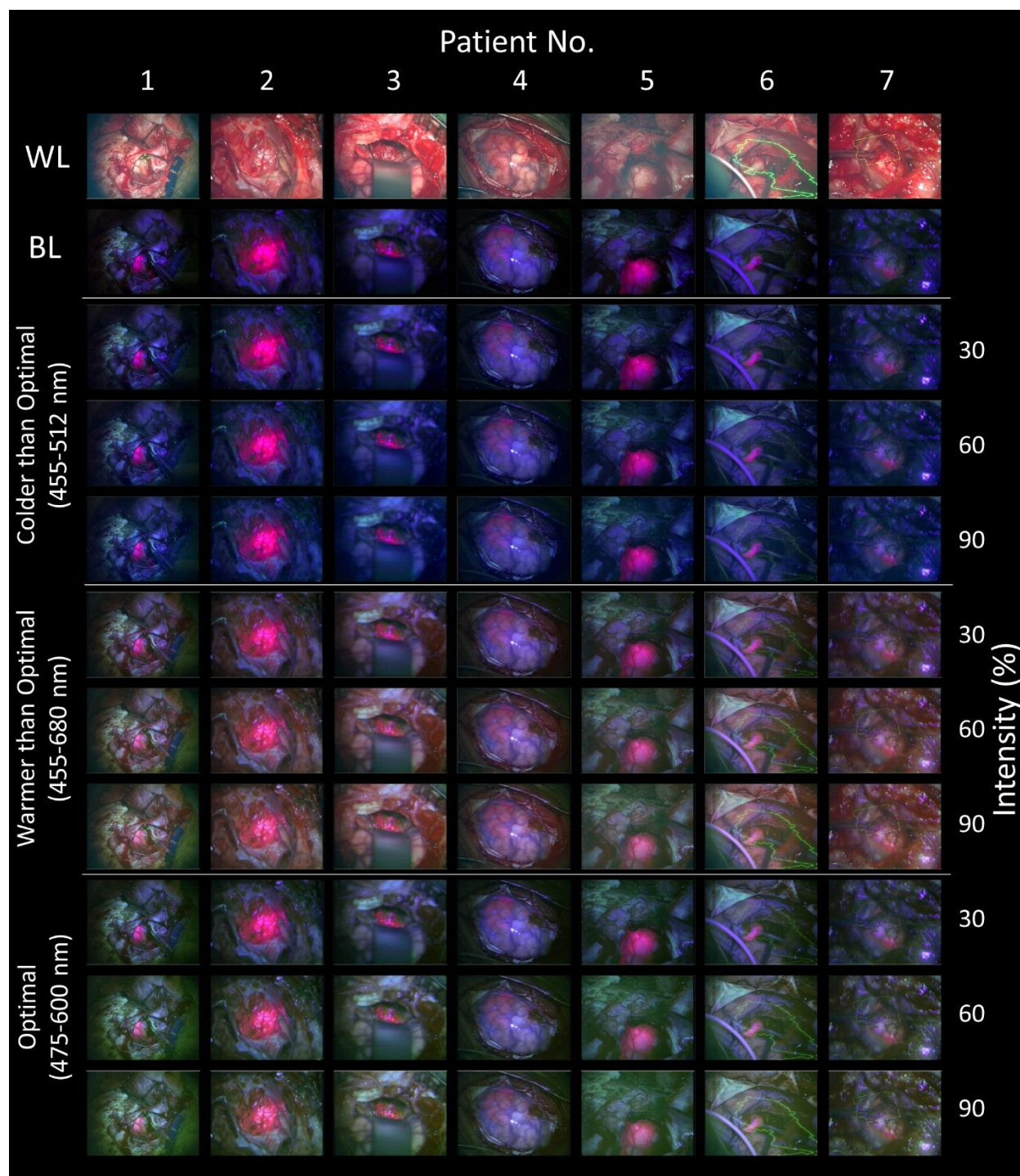
217 The tumor-to-background color contrast (TBCC) observed for different filter characteristics
218 exhibits a more complex relationship. To understand the impact of the illuminant on tumor-to-background
219 color, illuminants of different parameters were simulated using hyperspectral images acquired from
220 patients undergoing glioma. **Figure 1** briefly summarizes how these simulations were performed, and
221 once again, more details are provided in the Online Content. Patient images used to simulate the addition
222 of hypothetical light sources are shown in **Figure 4**. Little to no impact was observed on TBCC when
223 additional light of very cold temperature was added. However, as expected, the negative impact on TBCC
224 was strongest when the secondary illuminant spanned the red region of the spectrum and the PpIX
225 principle emission, causing light reflecting off the tissue to overlap with the tumor PpIX emission.

226 Since these two parameters work in opposition, the overall selection of filter and intensity is not
227 straight-forward. Since no direct means of mapping outcome to either TBCC or CRI, which would
228 provide a weighting factor, the optimal profile remains unknown. Based on our previously described CRI
229 and TBCC targets (CRI = 30, Δ TBCC < 15%), an optimal 475-600 nm spectral band was identified (see
230 Fig 1). Because the trade-off will sacrifice TBCC for CRI, the best strategy may be to allow the surgeon
231 to retain control of the intensity of the illuminant and select a secondary source with better CRI, which
232 will provide the flexibility needed for enhancing tumors which show a wide variability in the 5-ALA
233 signal intensity.

234

235

236



237

238 **Figure 4.** Images acquired under white-light (WL) and blue-light (BL) for seven patients undergoing craniotomy for
239 tumor resection with the addition of secondary illuminants (simulated) having different spectral properties (cool,
240 warm and optimal) at different intensities (3, 6, and 9).

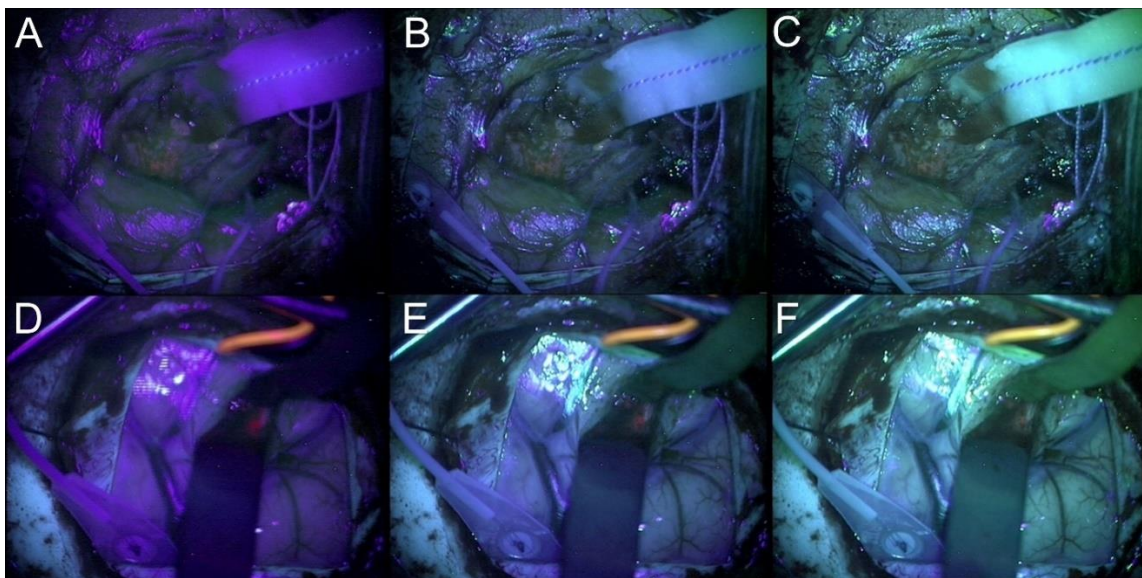
241

242

243 *Video Acquired During Fluorescence Guided Surgery using an Optimized Secondary Illuminant*

244 Two patients enrolled to receive 5-ALA FGR were imaged under blue light and white-light illumination
245 during the craniotomy procedure. These images were recorded under the same conditions (white-light
246 power of 30%, blue-light power of 100%, distance of 300 mm and magnification of 1.6x) as acquisitions
247 of the ColorChecker card (see ColorChecker Card Accuracy in Materials and Methods). The optimized
248 secondary illuminant, constructed with a 475 nm LPF and 600 nm SPF, was then used to illuminate the
249 surgical field during BLUE400 mode. Video showing the transition between BLUE400 and BLUE400 +
250 secondary illuminant (SI) was recorded (Online Content), and a panel of screen captures from the video
251 are presented in **Figure 5**.

252



253

254 **Figure 5.** Link to video. Images acquired during 5-ALA FGS from patient one (top row) and patient two (bottom
255 row) under blue light only, blue light with low secondary illumination, and blue light with medium secondary
256 illumination (left to right).

257 We set the maximum power of the secondary illuminant to 3x the irradiance of the blue light source
258 (48,000 lux). During deployment of the technology in the OR, about 30% of the maximum LED power
259 was used in the two patient cases summarized in **Figure 5**. In these surgeries, tumor exhibited lower
260 levels of PpIX fluorescence than in many of the cases shown in **Figure 4**; and therefore, they may not
261 represent conditions under which a secondary illuminant would provide the most added value.

262 Nevertheless, the surgeon (T.R.) reported that the secondary illuminant was able to highlight features that
263 were otherwise obscured in BLUE400 mode. This is observed in the video showing the transition from
264 white light to blue light to blue light with the SIA (**Video 1**, Online Content). In highly fluorescent

265 tumors, most of the surgery could be performed with the secondary light source on, although PpIX
266 fluorescence would only be visible if a carefully shaped spectrum was used.

267

268 Discussion

269 The salient finding of this paper is that, when considering the selection of a secondary illuminant to
270 improve the color rendering of the surgical field, the negative effect on tumor-to-background color
271 contrast is unavoidable. There is currently no outcomes data that would provide the impact of either CRI
272 improvement or TBCC degradation on disease-free progression, so no universal optimization is possible.
273 A secondary objective of this paper is to provide a framework to consider the impact of illumination on
274 appearance of tissue during surgery.

275 Given no global optimum exists across both CRI and TBCC, cost term weighting will impact the
276 overall optimization. In the absence of clinical outcome data—*e.g.*, how CRI influences avoidance of
277 critical structures like nerves and vessels, or how TBCC degradation impacts extent of tumor resection—
278 the weighting is arbitrary. Notwithstanding, we selected a CRI region corresponding to 30 for the purpose
279 of this study, which represents a light source with a color rendering quality better than a high-pressure
280 sodium light but worse than a fluorescent light. While these CRI values are below FDA guidelines, they
281 are common illuminants in day-to-day life. Determining the decrease in TBCC that would be tolerated is
282 more arbitrary. The largest decreases in contrast occurred when overlapping with the emission peak of
283 PpIX. Outside of this region, contrast was greatly improved. The selected filter-set produced about 15%
284 decrease in contrast. Once the filters were selected, the intensity of the light was varied, allowing the
285 surgeon to enhance contrast or the color rendering of the operative field as needed. It should be
286 emphasized that the “on the fly” adjustment can eliminate any degradation in TBCC by turning off the
287 secondary illuminant, but can only enhance CRI to a maximum of the CRI of the secondary light source
288 itself. Nevertheless, the ability to fine-tune the balance between improved CRI or improved TBCC
289 therefore allows individual surgeons to improve usability of 5-ALA, *e.g.*, at different phases of resection
290 within the same case, or for different cases where the concentration of 5-ALA induced PpIX fluorescence
291 might be bright enough to permit more secondary illumination. In this sense, the primary objective of this
292 paper to improve the usability of 5-ALA surgical guidance was achieved.

293 In a recent publication, Schwake et al. presented data where 5-ALA and fluorescein were used
294 simultaneously, remarking that the principle benefit of fluorescein was background illumination
295 facilitating visualization of the eloquent brain.¹⁸ The SIA would theoretically provide some of the same
296 benefits without the added task, cost and risk of administering another contrast agent. While its intensity
297 and spatial distribution could be controlled more effectively, a ‘frontlit’ approach like the SIA is more
298 likely to produce distracting specular reflections compared with the ‘backlit’ source provided by

299 fluorescein. It may also be argued that once the surgeon can effectively control the intensity of the SIA,
300 why not use a white-light SIA. Evidence from studies of human perception and cognition, suggest smooth
301 transition between BLUE400 and BLUE400+SI is more desirable than switching directly to white-light.
302 The ability to mentally integrate information from one representation of a scene into another, a type of
303 spatial reasoning, relies on qualitative aspects of the rendering (patterns, points of reference, landmarks)
304 to persist even when quantitative aspects of the image (chromaticity, brightness, object saliencies) change
305 18. The BLUE400 + SI mode may provide a rendering of the scene with more persistent aspects relative
306 to the BLUE400 mode, and therefore, may facilitate integrative spatial reasoning. The next step in this
307 technology development is to compare white-light and green-light SIAs to confirm whether there is an
308 added benefit to spatial reasoning.

309

310 **Conclusion**

311 This proof-of-concept paper demonstrates the use of a secondary illuminant adapter, affixed to
312 the bottom of a standard Zeiss Pentero operating microscope, to improve tissue color rendering during 5-
313 ALA FGR. The optimized light source balanced improvements in color rendering with reduction in 5-
314 ALA tumor-to-background contrast. Video of 5-ALA FGR acquired in two patients using the SIA is
315 shown to demonstrate the resulting effect on color rendering and contrast. While no global optimization
316 was possible since CRI and TBCC work in opposition when an SIA is added, the ability to allow surgeons
317 to individually, within the context of the phase of resection or patient-specific fluorescence properties,
318 modulate between enhanced TBCC and enhanced CRI provides substantive improvements in usability.

319

320 **Acknowledgements**

321 External funding for this work was provided by NIH/NCI R00 CA190890 and NIH/NCI RO1 NS052274.
322 The authors would also like to acknowledge internal funding support from the Dartmouth-Hitchcock
323 Medical Center's Department of Surgery and the Translational Engineering in Cancer Program at the
324 Norris Cotton Cancer Center.

325

326

327 **References**

328 1. Hefti, M. *et al.* 5-aminolaevulinic acid-induced protoporphyrin IX fluorescence in high-grade glioma
329 surgery. *Swiss medical weekly* **138**, 180–185 (2008).

- 330 2. Kamp, M. A. *et al.* 5-ALA fluorescence of cerebral metastases and its impact for the local-in-brain
331 progression. *Oncotarget* **7**, 66776 (2016).
- 332 3. Della Puppa, A. *et al.* 5-aminolevulinic acid (5-ALA) fluorescence guided surgery of high-grade
333 gliomas in eloquent areas assisted by functional mapping. Our experience and review of the
334 literature. *Acta neurochirurgica* **155**, 965–972 (2013).
- 335 4. Panciani, P. P. *et al.* 5-aminolevulinic acid and neuronavigation in high-grade glioma surgery: results
336 of a combined approach. *Neurocirugia* **23**, 23–28 (2012).
- 337 5. Stummer, W. *et al.* Fluorescence-guided resection of glioblastoma multiforme utilizing 5-ALA-
338 induced porphyrins: a prospective study in 52 consecutive patients. *Journal of neurosurgery* **93**,
339 1003–1013 (2000).
- 340 6. Millesi, M. *et al.* Analysis of the surgical benefits of 5-ALA–induced fluorescence in intracranial
341 meningiomas: experience in 204 meningiomas. *Journal of neurosurgery* **125**, 1408–1419 (2016).
- 342 7. Stummer, W. *et al.* Fluorescence-guided surgery with 5-aminolevulinic acid for resection of
343 malignant glioma: a randomised controlled multicentre phase III trial. *The lancet oncology* **7**, 392–
344 401 (2006).
- 345 8. Filbeck, T. *et al.* 5-aminolevulinic acid-induced fluorescence endoscopy applied at secondary
346 transurethral resection after conventional resection of primary superficial bladder tumors. *Urology*
347 **53**, 77–81 (1999).
- 348 9. Denzinger, S. *et al.* Clinically relevant reduction in risk of recurrence of superficial bladder cancer
349 using 5-aminolevulinic acid-induced fluorescence diagnosis: 8-year results of prospective
350 randomized study. *Urology* **69**, 675–679 (2007).
- 351 10. Atif, M. *et al.* Study of the efficacy of 5-ALA mediated photodynamic therapy on human
352 rhabdomyosarcoma cell line (RD). *Laser Physics Letters* **7**, 757 (2010).
- 353 11. Ewelt, C. *et al.* Cordectomy as final treatment option for diffuse intramedullary malignant glioma
354 using 5-ALA fluorescence-guided resection. *Clinical neurology and neurosurgery* **112**, 357–361
355 (2010).

- 356 12. Khursid, A. *et al.* Study of the efficacy of 5 ALA-mediated photodynamic therapy on human larynx
357 squamous cell carcinoma (Hep2c) cell line. *Laser physics* **20**, 1673–1678 (2010).
- 358 13. Roberts, D. W. *et al.* Red-light excitation of protoporphyrin IX fluorescence for subsurface tumor
359 detection. *Journal of neurosurgery* 1–8 (2017).
- 360 14. Bravo, J. J. *et al.* Hyperspectral data processing improves PpIX contrast during fluorescence guided
361 surgery of human brain tumors. *Scientific reports* **7**, 9455 (2017).
- 362 15. Valdés, P. A. *et al.* Quantitative fluorescence in intracranial tumor: implications for ALA-induced
363 PpIX as an intraoperative biomarker. *Journal of neurosurgery* **115**, 11–17 (2011).
- 364 16. Schanda, J. *Colorimetry: understanding the CIE system*. (John Wiley & Sons, 2007).
- 365 17. Sándor, N. & Schanda, J. Visual colour rendering based on colour difference evaluations. *Lighting*
366 *Research & Technology* **38**, 225–239 (2006).
- 367 18. Schwake, M., Stummer, W., Molina, E. J. S. & Wölfer, J. Simultaneous fluorescein sodium and 5-
368 ALA in fluorescence-guided glioma surgery. *Acta neurochirurgica* **157**, 877–879 (2015).

369

370

371

372

373